

Degenerated Liouvillians and steady-state reduced density matrices

Cite as: Chaos **31**, 073114 (2021); <https://doi.org/10.1063/5.0045308>

Submitted: 25 January 2021 . Accepted: 15 June 2021 . Published Online: 07 July 2021

 Juzar Thingna, and  Daniel Manzano

COLLECTIONS

Paper published as part of the special topic on [Dissipative Quantum Chaos](#)



View Online



Export Citation



CrossMark

ARTICLES YOU MAY BE INTERESTED IN

[A short introduction to the Lindblad master equation](#)

AIP Advances **10**, 025106 (2020); <https://doi.org/10.1063/1.5115323>

[Transient circulant clusters in two-population network of Kuramoto oscillators with different rules of coupling adaptation](#)

Chaos: An Interdisciplinary Journal of Nonlinear Science **31**, 073112 (2021); <https://doi.org/10.1063/5.0055578>

[Noise induced suppression of spiral waves in a hybrid FitzHugh–Nagumo neuron with discontinuous resetting](#)

Chaos: An Interdisciplinary Journal of Nonlinear Science **31**, 073117 (2021); <https://doi.org/10.1063/5.0059175>

Scilight

Summaries of the latest breakthroughs
in the **physical sciences**



Degenerated Liouvillians and steady-state reduced density matrices

Cite as: Chaos 31, 073114 (2021); doi: 10.1063/5.0045308

Submitted: 25 January 2021 · Accepted: 15 June 2021 ·

Published Online: 7 July 2021



View Online



Export Citation



CrossMark

Juzar Thingna^{1,2}  and Daniel Manzano^{3,a)} 

AFFILIATIONS

¹Center for Theoretical Physics of Complex Systems, Institute for Basic Science (IBS), Daejeon 34126, Republic of Korea

²Basic Science Program, University of Science and Technology, Daejeon 34113, Republic of Korea

³Departamento de Electromagnetismo y Física de la Materia and Instituto Carlos I de Física Teórica y Computacional, Universidad de Granada, Granada 18071, Spain

Note: This paper is part of the Focus Issue, Dissipative Quantum Chaos.

a) Author to whom correspondence should be addressed: manzano@onsager.ugr.es

ABSTRACT

Symmetries in an open quantum system lead to degenerated Liouvillians that physically imply the existence of multiple steady states. In such cases, obtaining the initial condition independent steady states is highly nontrivial since any linear combination of the *true* asymptotic states, which may not necessarily be a density matrix, is also a valid asymptote for the Liouvillian. Thus, in this work, we consider different approaches to obtain the *true* steady states of a degenerated Liouvillian. In the ideal scenario, when the open system symmetry operators are known, we show how these can be used to obtain the invariant subspaces of the Liouvillian and hence the steady states. We then discuss two other approaches that do not require any knowledge of the symmetry operators. These could be powerful numerical tools to deal with quantum many-body complex open systems. The first approach that is based on Gram–Schmidt orthonormalization of density matrices allows us to obtain *all* the steady states, whereas the second one based on large deviations allows us to obtain the non-degenerated maximum and minimum current carrying states. We discuss the symmetry-decomposition and the orthonormalization methods with the help of an open *para*-benzene ring and examine interesting scenarios such as the dynamical restoration of Hamiltonian symmetries in the long-time limit and apply the method to study the eigenspacing statistics of the nonequilibrium steady state.

Published under an exclusive license by AIP Publishing. <https://doi.org/10.1063/5.0045308>

In 1976, Gorini, Kossakowski, Sudarshan, and Lindblad (GKSL)^{1,2} independently proposed a completely positive trace preserving master equation that governs the dynamics of a generic quantum system. Since then, the equation has been a hallmark in the study of dissipative open quantum systems and has been used in a wider variety of applications. In recent years, due to the experimental advancements, engineering the bath properties and system–bath interaction has become possible. One immediate consequence is the existence of multiple steady states. In such cases, the dissipative Liouvillian becomes degenerated, having more than one invariant subspace. In general, finding the nonequilibrium steady states (NESSs) is highly nontrivial, and in this work, we outline three methods to address this issue. Each method has its own benefits and drawbacks. Using a *para*-benzene ring as an open quantum system, we elucidate the methods and find the existence of decoherence free subspaces or even dynamical restoration of Hamiltonian symmetries in the long-time limit. Last, since our

approach allows us to obtain the NESSs for a degenerated Liouvillian, we use it to study the statistics of the ratio of consecutive eigenspacing gaps r of the NESS, which shows the probability distribution $P(r) \rightarrow 0$ as $r \rightarrow 0$.

I. INTRODUCTION

Quantum master equations are an essential tool to study dissipative systems and have been applied to a wide variety of model systems in quantum optics,^{3–5} thermodynamics,^{6–10} transport,^{11–14} and quantum information.^{15,16} The most general Markovian master equation that preserves the properties of the density matrix (positivity, Hermiticity, and trace) is the Lindblad (or Gorini–Kossakowski–Sudarshan–Lindblad, GKSL) equation.^{1,2,17,18} This equation describes the dynamics of a system under the effect of a Markovian environment. The fixed points of this dynamics have

also been broadly analyzed. Evans¹⁹ proved that bounded systems present at least one fixed point and that there can be more than one leading to *degeneracy* of the Liouvillian.

The study of degenerated master equations has been very active during the last decade. The use of symmetries and degeneracy has been applied to reduce the dimensionality of open quantum systems,²⁰ to harness quantum transport,²¹ to detect magnetic fields,²² and in error correction.²³ In the timely field of quantum machine learning, there are approaches to pattern retrieval by the use of degenerated open quantum systems.²⁴ Furthermore, the non-equilibrium properties of molecular systems have been addressed to detect symmetries and multiple fixed points.²⁵

In the non-degenerated case, the initial condition independent steady state of a system can be obtained by numerically diagonalizing the dissipative Liouvillian. Unfortunately, the degenerated case is complicated because a linear combination of fixed points is also fixed, and thus, there is no guarantee that the diagonalization algorithm will return the physical steady states instead of their linear combinations. Thus, the problem of degenerated Liouvillians becomes nontrivial and hard to analyze numerically since the initial condition dependence cannot be easily eliminated.

In this paper, we present a toolbox for the extraction of the physical steady-states of degenerated open quantum systems in the Lindblad form. We present three different methods, a block diagonalization,²⁰ a Gram–Schmidt-inspired orthonormalization,²² and a method based in large deviation theory.²⁶ Each method has its own strengths and weaknesses. To illustrate the presented methods, we apply them to a model of a ring driven out of equilibrium by two thermal baths. We analytically calculate the steady-states, for a specific choice of the parameters, by the block-diagonalization method. We discuss the phenomenology of the open quantum system as a function of its bath parameters and test the numerical methods. The minimal model allows us to analytically discuss a plethora of interesting scenarios; e.g., we find that the invariant subspace of the Liouvillian can become degenerate if the bath is engineered to only pump energy into the system. In other words, even though one expects a single steady state corresponding to the invariant subspace, we find multiple steady states due to the dynamical degeneration of the invariant subspace. The Gram–Schmidt inspired method also allows us to explore the eigenspacing statistics of the nonequilibrium steady state (NESS) and understand the signatures from the perspective of random matrix theory.²⁷

This paper is organized as follows: In Sec. II, we discuss the main idea behind degenerated Liouvillians and symmetries in open quantum systems. Section III is dedicated to the general formulation of the three different methods to obtain the steady states. Particularly, Sec. III A deals with the block-diagonalization approach in which the open system symmetry operators are known. In Sec. III B, we discuss the Gram–Schmidt based orthonormalization procedure that allows us to obtain all the steady states, and Sec. III C is dedicated to the large deviation theory based method, which helps obtain the non-degenerate states carrying minimum or maximum current. In Sec. IV, we apply our different methods to a *para*-benzene ring, discuss analytically solvable cases, and study the eigenspacing statistics of the NESS. Finally, in Sec. V, we conclude and provide a future outlook.

II. DEGENERATED LIOUVILLIANS

In this section, we present the basics of degenerated Liouvillians and set up the notation that will be used in the paper. The main object of this study is mixed quantum states described by density matrices. If the Hilbert space of the pure states of our system is \mathcal{H} , then a mixed state is determined by a matrix $\rho \in O(\mathcal{H})$, with $O(\mathcal{H})$ being the space of bounded operators, that fulfills two properties,

$$\text{Normalization: } \text{Tr}(\rho) = 1,$$

$$\text{Positivity: } \rho > 0, \quad \text{i.e., } \forall |\psi\rangle \in \mathcal{H} \quad \langle \psi | \rho | \psi \rangle \geq 0. \quad (1)$$

Any matrix fulfilling these two properties is considered a density matrix. Another important concept we will use is orthogonality of density matrices. Two density matrices ρ_i and ρ_j are considered orthogonal if $\text{Tr}[\rho_i \rho_j] = 0$.

In this work, we consider the dynamics of the system to be governed by the Lindblad equation (see Ref. 18 for an introduction),

$$\begin{aligned} \frac{d\rho(t)}{dt} &= -i[H, \rho(t)] + \sum_i \left(L_i \rho(t) L_i^\dagger - \frac{1}{2} \{ \rho(t), L_i^\dagger L_i \} \right) \\ &\equiv \mathcal{L}[\rho(t)], \end{aligned} \quad (2)$$

where H is the Hamiltonian of our system of interest and L_i are positive bound operators called “jump operators.” Throughout this work, we will set $\hbar = k_B = 1$. The super-operator \mathcal{L} is usually named the *Liouville operator* of the system dynamics or just the *Liouvillian*. If the system pure states, \mathcal{H} , has a dimension N , the operator’s space dimension, $O(\mathcal{H})$, is N^2 . As the Lindblad equation represents a map of operators, the Liouvillian \mathcal{L} may be represented by a matrix of dimension $N^2 \times N^2$.

For bounded systems, Evans’ theorem states that this equation has at least one fixed point,¹⁹ meaning that there is at least one density matrix ρ such that

$$\text{Re}\{\mathcal{L}[\rho]\} = 0. \quad (3)$$

In most cases, there is at least one state such that $\mathcal{L}[\rho^{\text{SS}}] = 0$. These are called steady-states, and they do not evolve with time as $d\rho^{\text{SS}}/dt = \mathcal{L}[\rho^{\text{SS}}] = 0$. Evans’ theorem, as stated above, also includes the possibility of having pairs of states with a zero real part but a non-zero imaginary one.^{21,28} These states are called *stationary coherences*, and they evolve indefinitely.

The Liouvillian is a super-operator, and hence to obtain its spectrum, we need to map it to a matrix. The mathematical tool to do so is called the Fock–Liouville space (FLS). In the FLS, the density matrices are written as column vectors using an arbitrary map for its elements. All maps produce equivalent results, and hence, any choice of the map is a good choice. Once the density matrix is mapped to a column vector, the Liouvillian super-operator can be written as a $N^2 \times N^2$ general non-Hermitian matrix. It has both right and left eigenvectors, and its steady states (fixed points) correspond to the right eigenvectors with zero real eigenvalue.

Evans’ theorem also gives the conditions for obtaining a unique steady state.¹⁹ This happens iff the set of operators $\{H, L_i\}$ can generate the entire algebra of the space of bounded operators under multiplication and addition. In general, this condition is hard to prove for most systems (see Ref. 29 for an example). However, when not fulfilled, there are more than one steady states. This degeneracy

in the Liouvillian may be related to the presence of symmetries as we discuss in Sec. III.

Let us suppose that we have a degenerated Liouvillian with M zero eigenvalues (we suppose that there are no oscillating coherences). Each zero eigenvalue has an associated right-eigenvector that can be obtained by diagonalizing the Liouvillian expressed in the FLS. One could naïvely think that each of these right eigenvectors corresponds to a steady-state density matrix, but this is true only in very simple cases. In general, any linear combination of the steady-state density matrices is a right eigenvector of the Liouvillian with zero eigenvalue, but it is not necessarily a density matrix in the sense that may not be positive. Furthermore, it is also possible that the obtained right eigenvectors do not form an orthogonal set,³⁰ meaning that they do not belong to different invariant subspaces. Bearing these issues in mind, in Sec. III, we propose various approaches to obtain the steady-state density matrices, which are independent of initial conditions in each subspace of the Liouvillian.

III. METHODS TO OBTAIN STEADY STATES

We present three methods to calculate the steady-states of degenerated Liouvillians, the symmetry-decomposition, the orthonormalization, and the large deviation method. Each method has its own advantages. The symmetry-based one can be applied analytically for many cases and it is numerically cheap, but it requires full knowledge of the system’s symmetries. The orthonormalization can be applied with no previous knowledge about open system symmetries, but its computational cost increases with the degree of degeneracy. Finally, the large deviation method does not require previous knowledge about open system symmetries and it is computationally cheap, but it only gives the non-degenerated maximum and minimum current carrying states.

A. Diagonalization by symmetry-decomposition

In this subsection, we explain the relation between open system symmetry operators and multiple steady-states. We then use the knowledge of the symmetry operators and outline a procedure to obtain the steady states, some of which could have zero trace (non-physical density matrices).

To simplify our discussion, we focus on *strong* open system symmetries in which there exists a unitary operator π such that^{20,21}

$$[\pi, H] = [\pi, L_i] = 0 \quad \forall i. \tag{4}$$

This implies that the generators of the dissipative system dynamics $\{H, L_i\}$ and the symmetry operator π can be diagonalized with a common basis. Let us denote the eigenvalues of π as $v_i = e^{i\theta_i}$, with $i \in [1, n]$ and n being the number of distinct eigenvalues. Each eigenvalue can be degenerated, and hence, we introduce the index d_i that represents the dimension of the subspace corresponding to eigenvalue v_i . The corresponding eigenvectors of the symmetry operator π are $|v_i^\alpha\rangle$, with $i \in [1, n]$ and $1 \leq \alpha \leq d_i$.

We define a super-operator Π acting on the subspace of the bounded operators of \mathcal{H} as

$$\Pi[x] \equiv \pi \cdot x \cdot \pi^\dagger. \tag{5}$$

The spectrum of Π is derived from the one of π as

$$\Pi \left[|v_i^\alpha\rangle\langle v_j^\beta| \right] = e^{i(\theta_i - \theta_j)} |v_i^\alpha\rangle\langle v_j^\beta|. \tag{6}$$

Thus, the Hilbert space \mathcal{H} can be decomposed using the spectrum of π ,

$$\mathcal{H} = \bigoplus_{i=1}^n \mathcal{H}_i, \tag{7}$$

with $\mathcal{H}_i = \text{span} \{ |v_i^\alpha\rangle, \alpha = 1, \dots, d_i \}$. Similarly, the space of bounded operators \mathcal{B} can be expanded in the eigenspace of the super-operator Π as

$$\mathcal{B} = \bigoplus_{i,j=1}^n \mathcal{B}_{i,j}, \tag{8}$$

with $\mathcal{B}_{i,j} = \text{span} \{ |v_i^\alpha\rangle\langle v_j^\beta|, \alpha = 1, \dots, d_i; \beta = 1, \dots, d_j \}$. Using this decomposition, it is clear that these eigenspaces are invariant under the effect of the Liouvillian $\mathcal{L}[\mathcal{B}_{i,j}] \subseteq \mathcal{B}_{i,j}$. This implies that the Liouvillian can be block decomposed, using the basis of Π , into n^2 invariant subspaces.

Normalized density matrices are only possible in the subspaces $\mathcal{B}_{i,i}$, meaning that we have at least n steady states. It is also possible to find states having zero trace, belonging to the subspaces $\mathcal{B}_{i,j}$ ($i \neq j$).²² These states do not represent real density matrices, but they can form linear combinations with the steady states making physical differences. Note that we use the term “steady state” only for the states with finite trace and corresponding to zero eigenvalue of the Liouvillian. From the above description, it is also clear that steady states corresponding to different subspaces are orthogonal to each other.

The knowledge of a strong symmetry operator π gives us only a lower bound of the number of steady states. It is always possible that some of the blocks $\mathcal{B}_{i,i}$ are further degenerated. This happens when there are $K > 1$ strong symmetry operators, i.e., $\{\pi^{(1)}, \dots, \pi^{(K)}\}$ each of them with $n^{(j)}$ ($j = 1, \dots, K$) different eigenvalues such that³¹

$$[\pi^{(j)}, H] = [\pi^{(j)}, L_i] = [\pi^{(j)}, \pi^{(l)}] = 0 \quad \forall (i, j, l). \tag{9}$$

In this case, we can perform the block-diagonalization of the Liouvillian using the eigenbasis of $\pi^{(1)}$, obtaining

$$\mathcal{H} = \bigoplus_{i=1}^{n^{(1)}} \mathcal{H}_i. \tag{10}$$

Then, each block \mathcal{H}_i can be further block diagonalized into a maximum of $n^{(2)}$ blocks using the eigenbasis of $\pi^{(2)}$. This can be repeated until all symmetry operators are used. Thus, since the operation of each symmetry operator not always diagonalize the Liouvillian into exactly $n^{(j)}$ blocks, it is impossible to predict the total number of steady states. Thus, we can only impose bounds on the number of steady states M as $\max [n^{(j)}] < M < \prod_{l=1}^K n^{(l)}$.

To summarize the above outlined approach, we provide an algorithm to be applied to a system having K symmetry operators $\{\pi^{(j)}\}$ ($j = 1, \dots, K$). Each of the symmetry operators $\pi^{(j)}$ has $n^{(j)}$

distinct eigenvalues with phases $\{\theta_1^{(j)}, \theta_2^{(j)}, \dots, \theta_{n^{(j)}}^{(j)}\}$. As the symmetry operators commute with each other, we can define a common eigenbasis of all of them. The eigenbasis can be defined by the eigenvectors $\left\{ |v_{\theta_1^{(1)}, \theta_2^{(2)}, \dots, \theta_{i_K}^{(K)}}^\alpha \rangle \right\}$, where $i_j \in [1, n^{(j)}]$, and α stands for the degeneracy of the subspace determined by the eigenvalues $\theta_i = \{\theta_{i_1}^{(1)}, \theta_{i_2}^{(2)}, \dots, \theta_{i_K}^{(K)}\}$, where $\mathbf{i} = \{i_1, i_2, \dots, i_K\}$ and each element i_j of \mathbf{i} is associated with the same element $\theta^{(j)}$ of θ . This means that each vector $|v_{\theta_i}^\alpha\rangle$ is an eigenvector of each symmetry operator $\pi^{(j)}$; i.e.,

$$\pi^{(j)} |v_{\theta_i}^\alpha\rangle = \theta_{i_j}^{(j)} |v_{\theta_i}^\alpha\rangle. \tag{11}$$

The eigenbasis of the corresponding super-operators $\Pi^{(j)}$ is naturally given by the elements $\left\{ |v_{\theta_i}^\alpha\rangle \langle v_{\theta_{i'}}^\beta| \right\}$. The method to obtain the steady states of the degenerated Liouvillian, if we know its symmetry operators, is then

1. Find the common eigenbasis of all the symmetry operators $\{\pi^{(j)}\}$.
2. Calculate the eigenvalues of the symmetry operators corresponding to the elements of the basis, obtaining a classification of the form $|v_{\theta_i}^\alpha\rangle$.
3. Order the elements of the basis by grouping all the vectors with the same eigenvalues.
4. Change the Liouvillian to the new basis. A block-diagonal structure arises.
5. Diagonalize each block of the new basis. Any eigenvector with a zero eigenvalue corresponds to a steady state. Note that the dimension of the blocks is smaller than the dimension of the Liouvillian, and, therefore, the eigenvectors of the blocks do not represent density matrices by themselves.
6. Increase the dimension of the eigenvectors of each block by adding zeros to complete the dimension.
7. Change back to the original basis.

B. Diagonalization by orthonormalization

In Subsection III A, we dealt with the ideal scenario in which all the strong symmetry operators were known. In complex many-body open quantum systems, knowing all the strong symmetry operators is highly non-trivial, and the problem can become even more complicated if *weak* symmetry²⁰ is degenerating the Liouvillian. In this case, our starting point could be a set of M linearly independent right eigenvectors of the Liouvillian, which correspond to zero eigenvalue. One could naïvely expect that these operators are indeed the density matrices corresponding to the fixed points of the Liouvillian, but this is not the general case. In most cases, the diagonalization algorithm will give us a set of operators that are neither positive nor orthogonal to each other. Thus, in this subsection, we explain our second method to reconstruct the density matrices from such a set. This method was first presented in Ref. 22, and it does not require any pre-requisite knowledge of the strong or weak symmetry operators.

Having this objective in mind, the question we ask is: If we have a set of M zero eigenvalue eigenvectors of \mathcal{L} that are linearly independent $\{\tilde{\rho}_i\}$, how can we reconstruct M positive density matrices

$\{\rho_i\}$ with the following properties:

$$\mathcal{L}[\rho_i] = 0 \quad \forall i, \tag{12}$$

$$\text{Tr}[\rho_i \rho_j] = 0 \quad \forall i \neq j. \tag{13}$$

We will address this problem by a two-step approach. First, we construct a set of orthogonal matrices. To construct the orthonormal set, we start by applying an orthogonalization process based on the Gram-Schmidt algorithm. To begin, we form a set of Hermitian matrices $\{\rho_i^H\}$ from the original set,

$$\rho_i^H = \tilde{\rho}_i + \tilde{\rho}_i^\dagger. \tag{14}$$

Then, we use these Hermitian matrices $\{\rho_i^H\}$ to construct a set of orthogonal Hermitian matrices by applying

$$\begin{aligned} \rho_1^O &= \rho_1^H, \\ \rho_2^O &= \rho_2^H - \frac{\text{Tr}[\rho_1^O \rho_2^H]}{\text{Tr}[\rho_1^O \rho_1^O]} \rho_1^O, \\ \rho_3^O &= \rho_3^H - \frac{\text{Tr}[\rho_1^O \rho_3^H]}{\text{Tr}[\rho_1^O \rho_1^O]} \rho_1^O - \frac{\text{Tr}[\rho_2^O \rho_3^H]}{\text{Tr}[\rho_2^O \rho_2^O]} \rho_2^O, \\ &\vdots \\ \rho_M^O &= \rho_M^H - \sum_{j=1}^{M-1} \frac{\text{Tr}[\rho_j^O \rho_M^H]}{\text{Tr}[\rho_j^O \rho_j^O]} \rho_j^O. \end{aligned} \tag{15}$$

The orthonormalization process preserves Hermiticity, and it trivially follows that the set $\{\rho_i^O\}$ fulfill the orthogonality relation

$$\text{Tr}[\rho_i^O \rho_j^O] = 0 \quad \text{if } i \neq j. \tag{16}$$

This is a set of eigenmatrices of the Liouvillian with zero eigenvalue in which every matrix is Hermitian and orthogonal to each other. The only remaining issue is that these matrices may not be semi-positive definite, meaning that they may have negative eigenvalues. To address this issue, we first define the *positivity* functional, P , of a set of M Hermitian operators, $\{A_i\}_{i=1}^M$, of dimension N (the same as the dimension of density matrices) as

$$P[\{A_i\}] = \sum_{i=1}^M \sum_{j=1}^N \left(v_j^{A_i} - |v_j^{A_i}| \right), \tag{17}$$

with $v_j^{A_i}$ being the j th eigenvalue of operator A_i . It is clear that this measure is equal to zero iff all the matrices of the set $\{A_i\}_{i=1}^M$ are semi-positive definite. As the set of matrices $\{\rho_i^O\}_{i=1}^M$ are orthogonal and a linear combination of positive matrices, we may find a unitary operator, U , that transforms this set to zero eigenvalue positive orthogonal matrices $\{\rho_i^P\}$. To do so, we first write the original set as a column vector

$$|\rho^O\rangle \equiv \begin{pmatrix} \rho_1^O \\ \rho_2^O \\ \vdots \\ \rho_M^O \end{pmatrix}. \tag{18}$$

As we want to preserve orthogonality, we need to apply a unitary operator to the vector $|\rho^0\rangle$. Note here that each element of the vector $|\rho^0\rangle$ should be considered a point object. This transformation can be described by a set of $(M^2 - M)/2$ Euler angles, $\chi = \{\chi_1, \chi_2, \dots, \chi_{\frac{M^2-M}{2}}\}$. For a specific choice of the Euler angles, we can define the new vector of matrices $|\rho(\chi)\rangle = U(\chi)|\rho^0\rangle$, corresponding to the set of matrices $\{\rho_i(\chi)\}$. For example, if we have three steady states, i.e., $M = 3$, then we have three $[(M^2 - M)/2]$ Euler angles, and one possible form of the general rotation matrix in three dimensions is given by

$$U(\chi) = \begin{pmatrix} c_1c_3 - c_2s_1s_3 & -c_1s_3 - c_2c_3s_1 & s_1s_2 \\ c_3s_1 + c_1c_2s_3 & c_1c_2c_3 - s_1s_3 & -c_1s_2 \\ s_1s_3 & c_3s_2 & c_2 \end{pmatrix}, \quad (19)$$

where s and c represent sine and cosine and the subscripts 1, 2, and 3 represent χ_1, χ_2 , and χ_3 , i.e., $c_1 = \cos(\chi_1)$, on the right hand side. The Euler angles lie within the range $0 \leq \chi_1, 0 \leq \chi_2 \leq \pi$, and $\chi_3 < 2\pi$. Thus, using the ρ_i^0 as point objects, we can obtain the set of matrices $\{\rho_i(\chi_1, \chi_2, \chi_3)\}$.

In order to find the correct choice of the angles that performs the correct transformation, we need to maximize the functional

$$P[\{\rho_i(\chi)\}] = \sum_{i=1}^M \sum_{j=1}^N \left(v_j^{\rho_i(\chi)} - |v_j^{\rho_i(\chi)}| \right), \quad (20)$$

with respect to the various Euler angles. Thus, we can obtain a set of orthogonal semi-definite positive zero eigenvalue right-eigenvector matrices $\{\rho_i^p\}$. These obtained matrices need not be normalized, and this can be easily achieved by transforming $\rho_i = \rho_i^p / \text{Tr}[\rho_i^p]$ for all the matrices that have $\text{Tr}[\rho_i^p] \neq 0$.

The above described method can be summarized as follows:

1. Obtain a set of Hermitian matrices by applying Eq. (14) and obtaining the set $\{\rho_i^H\}$.
2. Construct a set of orthogonal matrices, $\{\rho_i^O\}$, by applying a Gram-Schmidt method for density matrices.
3. Find the rotation angles, $\chi = \{\chi_1, \chi_2, \dots, \chi_{\frac{M^2-M}{2}}\}$, by maximizing the functional, Eq. (20).
4. Apply the rotation $U(\chi)$ to obtain the orthonormal semi-positive definite Hermitian set of matrices $\{\rho_i^p\}$.
5. Renormalize by doing $\rho_i = \rho_i^p / \text{Tr}[\rho_i^p]$ for all the matrices that have $\text{Tr}[\rho_i^p] \neq 0$.

C. Diagonalization by large deviations

In this subsection, we describe a method to obtain some of the steady states by a single diagonalization of the Liouvillian, making it much simpler than the previous methods. On the other hand, it can be applied only in some cases, and it allows us to obtain only some of the states. The method is based on the study of the thermodynamic currents, and it was first presented in Ref. 26 (see Ref. 21 for a more detailed discussion). Here, we focus only on the description of this approach and its applicability.

We consider a system connected to several incoherent channels that allow the exchange of quanta between the system and an environment. This allows us to divide the super-operator \mathcal{L} from Eq. (2)

into three parts,

$$\mathcal{L} = \mathcal{L}_{-1} + \mathcal{L}_0 + \mathcal{L}_{+1}, \quad (21)$$

where the subscripts indicate the number of excitations introduced/removed from the system by the environment. Of course, there could be more exotic environments that exchange more than one excitation, but for the sake of simplicity, we will not consider this possibility. Next, we define the system density matrix conditioned on a fixed number of excitations Q as $\rho_Q(t) \equiv \text{Tr}_Q[\rho(t)]$, where Tr_Q is partial trace over the manifold containing Q excitations. Thus, the evolution of $\rho_Q(t)$ is governed by

$$\frac{d\rho_Q(t)}{dt} = \mathcal{L}_{-1}[\rho_{Q+1}(t)] + \mathcal{L}_0[\rho_Q(t)] + \mathcal{L}_{+1}[\rho_{Q-1}(t)]. \quad (22)$$

This gives a hierarchy of equations that can be unraveled using the Laplace transform

$$\rho_\lambda(t) = \sum_{Q=-\infty}^{\infty} \rho_Q(t) e^{-\lambda Q}, \quad (23)$$

which when applied to Eq. (22) gives a set of independent equations

$$\begin{aligned} \frac{d\rho_\lambda(t)}{dt} &= e^\lambda \mathcal{L}_{-1}[\rho_\lambda(t)] + \mathcal{L}_0[\rho_\lambda(t)] + e^{-\lambda} \mathcal{L}_{+1}[\rho_\lambda(t)] \\ &\equiv \mathcal{L}_\lambda[\rho_\lambda(t)], \end{aligned} \quad (24)$$

where λ is known as the *counting field*. For the Lindblad equation that takes the form of Eq. (2), we have the correspondence

$$\begin{aligned} \mathcal{L}_{-1}[\rho(t)] &= L_i \rho(t) L_i^\dagger, \\ \mathcal{L}_{+1}[\rho(t)] &= L_j \rho(t) L_j^\dagger, \\ \mathcal{L}_0[\rho(t)] &= -i[H, \rho(t)] \\ &\quad + \sum_{k \neq ij} L_k \rho(t) L_k^\dagger - \frac{1}{2} \sum_k \{L_k L_k^\dagger, \rho(t)\}, \end{aligned} \quad (25)$$

where the index i/j stand for the incoherent channels that extract/inject excitations in the system. The probability of finding the system in a state with Q excitations is $P_Q(t) = \text{Tr}[\rho_Q(t)]$, and

$$Z_\lambda(t) \equiv \text{Tr}[\rho_\lambda(t)] = \sum_{Q=-\infty}^{\infty} P_Q(t) e^{-\lambda Q} \quad (26)$$

is known as the generating function of the current probability distribution. This generating function follows a *large deviation principle*, and for a long time, it scales as

$$Z_\lambda(t) \sim e^{t\mu(\lambda)}, \quad (27)$$

where $\mu(\lambda)$ is called the current *Large Deviation Function* (LDF). It can be calculated as the highest eigenvalue of the tilted super-operator \mathcal{L}_λ . As $Z_\lambda(t)$ is the current moment generating function, the LDF μ_λ corresponds to the cumulant generating function of the current distribution. Therefore, the average current can be

calculated as

$$\langle \dot{Q} \rangle = \lim_{t \rightarrow \infty} \frac{1}{t} \left. \frac{\partial Z_\lambda(t)}{\partial \lambda} \right|_{\lambda=0} = \left. \frac{\partial \mu(\lambda)}{\partial \lambda} \right|_{\lambda=0}. \quad (28)$$

If $|\lambda| \ll 1$, we can expand the LDF as

$$\mu(\lambda)|_{\lambda \rightarrow 0} \sim \mu(0) + \lambda \left. \frac{\partial \mu(\lambda)}{\partial \lambda} \right|_{\lambda=0} = \langle \dot{Q} \rangle. \quad (29)$$

Therefore, if the Liouvillian is degenerated and the different steady states have non-degenerated average currents, the LDF $\mu(\lambda)$ will have a non-analytic behavior around $\lambda = 0$ in the form

$$\mu(\lambda) = \begin{cases} +|\lambda| \langle \dot{Q} \rangle_{\max} & \text{for } \lambda \rightarrow 0^-, \\ -|\lambda| \langle \dot{Q} \rangle_{\min} & \text{for } \lambda \rightarrow 0^+. \end{cases} \quad (30)$$

This allows us to calculate the steady-states corresponding to the maximum and minimum currents as long as they are not degenerated. The method may be summarized as follows:

1. Calculate the highest eigenvalue $\mu(\lambda)$ (and its corresponding eigenvector ρ_λ) of the modified Liouvillian \mathcal{L}_λ .
2. Take the limits $\rho'_{\min} = \lim_{\lambda \rightarrow 0^+} \rho_\lambda$ and $\rho'_{\max} = \lim_{\lambda \rightarrow 0^-} \rho_\lambda$.
3. Renormalize, obtaining $\rho_{\min} = \rho'_{\min} / \text{Tr}[\rho'_{\min}]$ and $\rho_{\max} = \rho'_{\max} / \text{Tr}[\rho'_{\max}]$.

To summarize this section, we have introduced three different methods using which we can obtain the steady states for an open quantum system with a degenerated Liouvillian. The first method described in Sec. III A is the most general approach but requires the knowledge of symmetry operators that are usually difficult to obtain. The second approach (Sec. III B) could be easily implemented computationally and does not require any knowledge of the symmetry operators. Although this seems most beneficial, with an increase in the degree of degeneracy, the computational cost increases substantially due to the minimization procedure to find the optimal Euler angles. The final method is the easiest computationally (Sec. III C) but is limited to a class of nonequilibrium systems and can be used to obtain only a subset of the steady states.

IV. EXAMPLE: PARA-BENZENE RING

The methods presented can deal with a wide variety of scenarios, and in order to illustrate these, we use the example of a *para*-benzene ring connected to two reservoirs as illustrated in Fig. 1. We restrict to the single-excitation picture and consider the Hilbert space to be spanned by the site basis $\{|\tilde{i}\rangle\}_{i=1}^6$ plus a ground state $|\tilde{0}\rangle$ to allow interactions with the reservoir. The system Hamiltonian takes the form

$$H = J \sum_{\tilde{n}=1}^6 |\tilde{n}\rangle \langle \tilde{n}+1| + \text{H.c.}, \quad (31)$$

with $|\tilde{7}\rangle = |\tilde{1}\rangle$. The system is boundary driven by two incoherent baths connected to sites 1 and 4. The baths exchange energy and

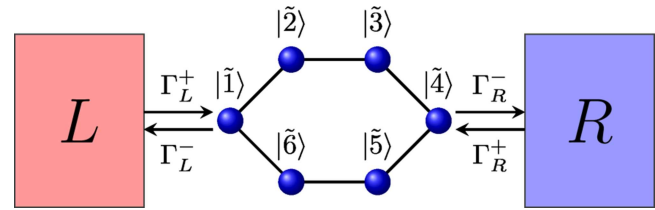


FIG. 1. Illustration of the *para*-benzene-type system with six sites connected to two incoherent baths (red and blue rectangles) at different temperatures T_L and T_R . The *para*-benzene system exchanges energy with the left L and right R baths due to the pumping rates Γ^+ and dumping rates Γ^- . The tilde basis is the original site representation.

excitations with the system via the jump operators

$$\begin{aligned} L_1 &= \sqrt{\Gamma_L^+} |\tilde{1}\rangle \langle \tilde{0}|, & L_2 &= \sqrt{\Gamma_L^-} |\tilde{0}\rangle \langle \tilde{1}|, \\ L_3 &= \sqrt{\Gamma_R^+} |\tilde{4}\rangle \langle \tilde{0}|, & L_4 &= \sqrt{\Gamma_R^-} |\tilde{0}\rangle \langle \tilde{4}|, \end{aligned} \quad (32)$$

where $\Gamma_x^{+(-)} \geq 0$ are the pumping (dumping) rates for the x th bath ($x = L$ or R). All properties of the baths are encoded in these rates, and we will not consider any specific form herein. The model here is a simple model to elucidate the idea of a degenerated Liouvillian, and our primary focus is to demonstrate the mathematical framework of symmetries in open quantum systems. Readers might be interested in applying such models to understand nonequilibrium observables such as heat currents, but with such local master equations, one needs to define the thermodynamic observables carefully³² in order to avoid violations of thermodynamic laws or use non-Lindblad master equations (like Redfield) that can be precisely mapped to a microscopic model.³³

For the simple ring structure, there is only one open system symmetry operator given by

$$\pi = \sum_{i=0,1,4} |\tilde{i}\rangle \langle \tilde{i}| + |\tilde{2}\rangle \langle \tilde{6}| + |\tilde{6}\rangle \langle \tilde{2}| + |\tilde{3}\rangle \langle \tilde{5}| + |\tilde{5}\rangle \langle \tilde{3}|. \quad (33)$$

The unitary operator π has two eigenvalues $+1$ and -1 , and the transformation matrix T to change basis from the site representation to the eigenvectors $|i\rangle$ of π reads

$$\begin{aligned} T |\tilde{i}\rangle &= |i\rangle, \\ T &= \sum_{i=0,1,4} |\tilde{i}\rangle \langle \tilde{i}| + \frac{1}{\sqrt{2}} \sum_{i=2,3} |\tilde{i}\rangle \langle \tilde{i}| - \frac{1}{\sqrt{2}} \sum_{i=5,6} |\tilde{i}\rangle \langle \tilde{i}| \\ &\quad + \frac{1}{\sqrt{2}} (|\tilde{2}\rangle \langle \tilde{6}| + |\tilde{3}\rangle \langle \tilde{5}| + \text{H.c.}). \end{aligned} \quad (34)$$

The ground $|0\rangle$ and symmetric states $|i\rangle$ ($i = 1, \dots, 4$) have eigenvalue $+1$, whereas the anti-symmetric states $|i\rangle$ ($i = 5, 6$) correspond to eigenvalue -1 . The transformation matrix does not affect the ground $|\tilde{0}\rangle$ and *edge* sites ($\tilde{1}$ and $\tilde{4}$), which are connected to the baths but only transforms the *bulk* sites ($\tilde{2}, \tilde{3}, \tilde{5}$, and $\tilde{6}$).

The system Hamiltonian in the transformed basis takes the form

$$H = \sqrt{2}J(|1\rangle\langle 2| + |3\rangle\langle 4|) + J(|2\rangle\langle 3| + |5\rangle\langle 6|) + \text{h.c.}, \quad (35)$$

which is block diagonal since the ground and symmetric subspace ($|0\rangle, \dots, |4\rangle$) does not interact with the anti-symmetric one ($|5\rangle$ and $|6\rangle$). Since the transformation does not affect the ground state and the edge sites, there is no entanglement generated in the jump operators and they remain the same form as Eq. (32) with $|\bar{i}\rangle \rightarrow |i\rangle$.

Given the block-diagonal form of the system Hamiltonian and the jump operators confined to the ground and symmetric subspace, we can split the system space into the subspace of the ground state (\mathcal{H}_g with one state), symmetric states (\mathcal{H}_s with four states), and anti-symmetric states (\mathcal{H}_a with two states). Thus, the system Hamiltonian can be decomposed into a 3×3 matrix that takes the form

$$H = \begin{pmatrix} 0 & 0 & 0 \\ 0 & H_{ss} & 0 \\ 0 & 0 & H_{aa} \end{pmatrix}. \quad (36)$$

In this representation, the sum of the jump operators takes the form

$$\sum_{i=1}^4 L_i = \begin{pmatrix} 0 & L_- & 0 \\ L_+ & 0 & 0 \\ 0 & 0 & 0 \end{pmatrix}, \quad (37)$$

with $L_+ = L_1 + L_3$ representing the net pumping operator and $L_- = L_2 + L_4$ being the net dumping operator. The Lindblad equation (2) then separates out for each sub-block, and the resultant equations read

$$\begin{aligned} \frac{d\rho_{gg}(t)}{dt} &= -\frac{1}{2}\{N_+, \rho_{gg}(t)\} + L_- \rho_{ss}(t) L_-^\dagger, \\ \frac{d\rho_{ss}(t)}{dt} &= -i[H_{ss}, \rho_{ss}(t)] - \frac{1}{2}\{N_-, \rho_{ss}(t)\} \\ &\quad + L_+ \rho_{gg}(t) L_+^\dagger, \end{aligned} \quad (38)$$

$$\begin{aligned} \frac{d\rho_{gs}(t)}{dt} &= i\rho_{gs}(t)H_{ss} - \frac{1}{2}\rho_{gs}(t)N_- - \frac{1}{2}N_+\rho_{gs}(t), \\ \frac{d\rho_{ga}(t)}{dt} &= i\rho_{ga}(t)H_{aa} - \frac{1}{2}N_+\rho_{ga}(t), \\ \frac{d\rho_{sa}(t)}{dt} &= -i(H_{ss}\rho_{sa}(t) - \rho_{sa}(t)H_{aa}) - \frac{1}{2}N_-\rho_{sa}(t), \end{aligned} \quad (39)$$

$$\frac{d\rho_{aa}(t)}{dt} = -i[H_{aa}, \rho_{aa}(t)], \quad (40)$$

with $N_+ = L_+^\dagger L_+$ and $N_- = L_-^\dagger L_-$ being positive operators and $\rho_{x,y}(t) = \rho_{y,x}^\dagger(t)$ ($\{x, y\} = g, s, a$). The cross-subspaces, i.e., $\rho_{x,y}(t) \forall x \neq y$, the reduced density matrix $\rho_{x,y}(t)$ decays exponentially as can be seen from Eq. (39).

Thus, in the steady state, only the diagonal components of the reduced density matrix survive, and we now focus on the anti-symmetric subspace whose evolution is described by Eq. (40). Clearly, this describes coherent evolution, and thus, the anti-symmetric subspace is a decoherence free subspace. The

eigenvectors of H_{aa} (2×2 matrix) can be easily obtained and are given by

$$\begin{aligned} |\psi_1\rangle &= \frac{1}{\sqrt{2}}(|5\rangle + |6\rangle), \\ |\psi_2\rangle &= \frac{1}{\sqrt{2}}(|5\rangle - |6\rangle). \end{aligned} \quad (41)$$

If we initiate our system in any one of these states, it will not evolve in time, and hence, from the perspective of the general Lindblad equation, both of these pure states are steady states. In other words, the dark states

$$\rho_1^{\text{DS}} = |\psi_1\rangle\langle\psi_1| \quad \text{and} \quad \rho_2^{\text{DS}} = |\psi_2\rangle\langle\psi_2| \quad (42)$$

are zero current carrying steady states. The cross combination of these states displays oscillating behavior and is known as oscillating coherences²⁸ whose state has zero trace $\rho^{\text{OC}}(t) = e^{-i2Jt}|\psi_1\rangle\langle\psi_2| + e^{i2Jt}|\psi_2\rangle\langle\psi_1|$. The frequency of the oscillations is given by the difference of the eigenvalues of H_{aa} . Thus, the existence of decoherence free subspaces always gives us L number of steady states, where L is the dimension of the decoherence free subspace, and L pairs of eigenvalues of the Liouvillian with zero real part but a finite imaginary part known as oscillating coherences.

The reduced density matrix for the subspaces belonging to the ground and symmetric states obeys coupled first order differential equations [see Eq. (38)], which is impossible to solve analytically. In general, this setup has *three* steady states; one from the ground and symmetric subspace and two from the anti-symmetric subspace described above. In specific scenarios, wherein the effect of the bath can be simplified, we can obtain analytic solutions as described below.

A. Equilibrium

We can simplify our problem by considering that the pumping (dumping) rates of both baths are the same; i.e., $\Gamma_L^+ = \Gamma_R^+ = \Gamma$ and $\Gamma_L^- = \Gamma_R^- = \gamma$. In this case, the equilibrium steady state is given by

$$\rho_3^{\text{EQ}} = \frac{\gamma}{\gamma + 4\Gamma}|0\rangle\langle 0| + \frac{\Gamma}{\gamma + 4\Gamma} \sum_{i=1}^4 |i\rangle\langle i|. \quad (43)$$

If the baths were ideal sinks $\Gamma = 0$ (zero temperature baths) or pumping and dumping at the same rate $\gamma = \Gamma$ (infinite temperature baths), we obtain the physically intuitive results of either being localized in the ground state or all states being equally populated. Note here that in the general equilibrium scenario, we do not obtain the canonical Gibbs state because the jump operators in our Lindblad equation are resonantly being coupled to the ground state $\tilde{0}$ and either site $\tilde{1}$ or $\tilde{4}$. Such a resonant coupling does not allow the dissipator to mix *all* the energy levels, which is a crucial requirement to obtain a Gibbsian state at equilibrium.

B. Ideal source

In another extreme scenario when the baths are an ideal source such that $\Gamma_L^+ = \Gamma_R^+ = \Gamma$ and $\Gamma_L^- = \Gamma_R^- = 0$, the dynamical

equations of the ground-symmetric subspace [Eq. (38)] simplify as

$$\frac{d\rho_{gg}(t)}{dt} = -2\Gamma\rho_{gg}(t), \quad (44)$$

$$\frac{d\rho_{ss}(t)}{dt} = -i[H_{ss}, \rho_{ss}(t)] + \Gamma\rho_{gg}(t) \sum_{ij=1,4} |i\rangle\langle j|. \quad (45)$$

The equation for $\rho_{gg}(t)$ can be solved analytically giving an exponentially decaying solution $\rho_{gg}(t) = \exp[-2\Gamma t]\rho_{gg}(0)$ with $\rho_{gg}(0)$ being the initial condition. In the long-time limit, $\rho_{gg} = 0$, which is expected since the baths only pump excitations from the ground state to the ring. In this long-time limit, it is clear from Eq. (45) that $\rho_{ss}(t)$ obeys an oscillatory coherent evolution. Thus, in this ideal-source limit, we obtain more than three steady states (six in particular): the anti-symmetric subspace is not affected by this analysis and hence gives the two steady states as explained above, whereas the ground and symmetric subspace now gives *four* (dimension of H_{ss}) steady states using the same arguments we provided for the coherent evolution in the anti-symmetric subspace analysis. Note here that the emergence of these extra steady states is not due to the open system symmetries but because there was a dynamical restoration of Hamiltonian symmetries in the long-time limit.

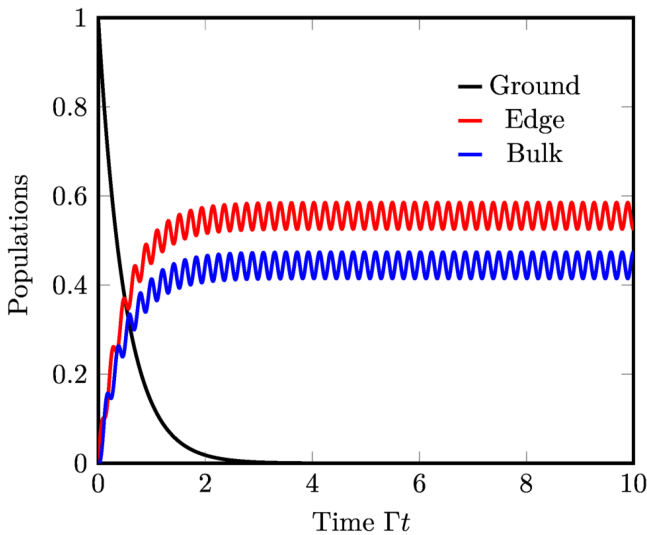


FIG. 2. Populations as a function of time t for the case of pure pumping $L^-_i = 0$. The system exhibits a dynamical decoherence free subspace due to which we obtain multiple steady states even in the absence of strong or weak open system symmetries. The symmetric subspace is invariant, and only in the limit $t \rightarrow \infty$, the invariant symmetric subspace becomes decoherence free. The ground state population is $\langle \tilde{0} | \rho(t) | \tilde{0} \rangle$, the edge state population is $\rho_{\text{edge}}(t) = \sum_{i=1,4} \langle \tilde{i} | \rho(t) | \tilde{i} \rangle$, and the bulk state population is $\rho_{\text{bulk}}(t) = \sum_{i=2,3,5,6} \langle \tilde{i} | \rho(t) | \tilde{i} \rangle$. All individual sites in the bulk or edge have the same populations due to the open system symmetries, and the difference in the bulk and edge site populations is due to the symmetries in H_{ss} . The pumping rate for both baths $\Gamma^+_{\alpha} = \Gamma = 0.1$ and the hopping $J = 1$.

Thus, in general, the existence of multiple steady states need not be rooted in open system symmetries (as usually believed) but could arise due to the peculiar properties of the baths.

We illustrate this evolution for the real-space populations in Fig. 2. The ground state (black solid line) population decays exponentially as expected, and the populations of the edge [$\rho_{\text{edge}}(t) = \sum_{i=1,4} \langle \tilde{i} | \rho(t) | \tilde{i} \rangle$, red solid line] and bulk [$\rho_{\text{bulk}}(t) = \sum_{i=2,3,5,6} \langle \tilde{i} | \rho(t) | \tilde{i} \rangle$, blue solid line] sites oscillate indefinitely. The oscillations of the edge and bulk are out of phase, and the difference in their amplitudes is due to the symmetries in H_{ss} , which has different weights for the connections between the edges and bulk sites [see Eq. (35)].

C. Ideal sink and source

Next, we turn our attention to systems in nonequilibrium. The simplest case that yields analytic results is when one of the baths is an ideal sink $\Gamma^+_L = 0$, $\Gamma^-_L = \gamma$, whereas the other is an ideal source $\Gamma^+_R = \Gamma$, $\Gamma^-_R = 0$. Unlike the ideal-source scenario, in which the ground state gets depleted leading to dynamical restoration of Hamiltonian symmetries, in this case, the ideal sink would re-populate the ground state ensuring that a current carrying NESS exists. The ground and symmetric subspace has only one NESS given by

$$\begin{aligned} \rho_3^{\text{NESS}} = & \frac{1}{1 + \frac{4\Gamma}{\gamma} + \frac{9\gamma\Gamma}{16J^2}} \left\{ |0\rangle\langle 0| + \frac{\Gamma}{\gamma} |1\rangle\langle 1| + \left(\frac{\Gamma}{\gamma} + \frac{\gamma\Gamma}{8J^2} \right) |2\rangle\langle 2| \right. \\ & + \left(\frac{\Gamma}{\gamma} + \frac{\gamma\Gamma}{4J^2} \right) |3\rangle\langle 3| + \left(\frac{\Gamma}{\gamma} + \frac{3\gamma\Gamma}{16J^2} \right) |4\rangle\langle 4| \\ & - i \frac{\Gamma}{2\sqrt{2}J} \left(|1\rangle\langle 2| + \sqrt{2} |1\rangle\langle 4| + \frac{1}{\sqrt{2}} |2\rangle\langle 3| \right. \\ & \left. \left. - i \frac{4J}{\gamma} |2\rangle\langle 4| + |3\rangle\langle 4| + \text{H.c.} \right) \right\}. \quad (46) \end{aligned}$$

The steady-state excitonic current for the ideal sink source scenario is

$$\begin{aligned} I_L = & \text{Tr}[L^\dagger_1 L_1 \rho_3^{\text{NESS}}] - \text{Tr}[L^\dagger_2 L_2 \rho_3^{\text{NESS}}] \\ = & \frac{\Gamma}{1 + \frac{4\Gamma}{\gamma} + \frac{9\gamma\Gamma}{16J^2}}. \quad (47) \end{aligned}$$

D. General case

In the general nonequilibrium case, it is not possible to solve the differential equations exactly, and hence, we solve these numerically and display the dynamics in Fig. 3. The solid lines in Fig. 3 are for the low temperature regime in which we find that the edge (red lines) and bulk (blue lines) state populations are different. The difference in the populations can be attributed to the symmetries of the symmetric subspace Hamiltonian H_{ss} (recall a similar behavior was observed in the ideal-source case). At low temperatures, the bath should not affect the system dramatically, and thus, the Hamiltonian symmetries should be respected. On the other hand, at high temperatures (Fig. 3, dashed lines), the dissipative baths completely alter the system dynamics, and hence, in this case, we do not see any

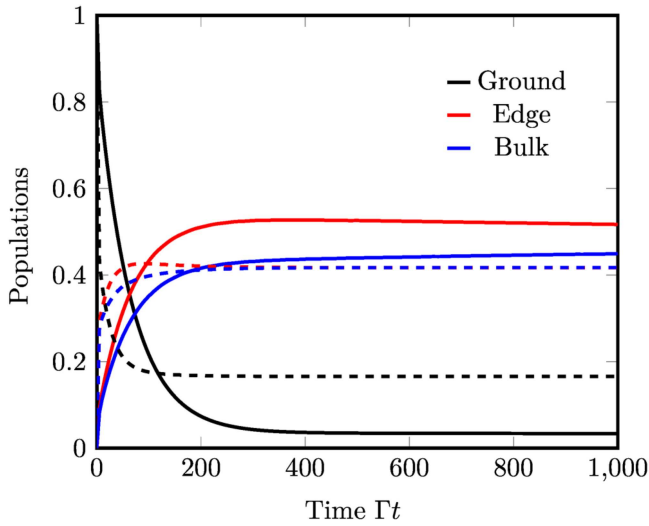


FIG. 3. Populations as a function of time t for the general nonequilibrium scenario. Solid lines are for the case of low temperature with $T_L = 0.25$ and $T_R = 0.5$, whereas dashed lines are for the high temperature regime with $T_L = 1$ and $T_R = 2$. The individual edge and bulk sites (the same as that defined in the caption of Fig. 2) have the same populations due to open system symmetries. At low temperatures, the edge and bulk populations are distinct exhibiting the same symmetry governed by H_{ss} (the same as Fig. 2). At high temperatures, the Hamiltonian symmetry is broken, and the bulk and edge site populations become equal after a short transient. The hopping is chosen to be $J = 1$, and the rates obey local-detailed balance, $\Gamma_x^+ = \Gamma \omega_0 n(T_x, \omega_0)/2$ and $\Gamma_x^- = \Gamma \omega_0 [1 + n(T_x, \omega_0)]/2$ with $x = L, R$, $n(T, \omega_0) = [\exp(\omega_0/T) - 1]^{-1}$ being the Bose-Einstein distribution, $\omega_0 = 1$ being the system-bath resonant frequency, and $\Gamma = 0.1$ the system-bath coupling strength.

signatures of the H_{ss} symmetries being preserved. In fact, at high temperatures, the edge and bulk populations become equal after a short transient, indicating an equal distribution of the excitation among the edge and bulk.

E. Eigenspacing statistics of NESS

There are several scenarios in which knowing the NESS for a degenerated Liouvillian could be useful. In this subsection, we focus on the timely example of studying the eigenspacing statistics of the NESS as first proposed in Ref. 27. Recently, there has been a surge in understanding the universal properties of a dissipative open quantum system mostly restricted to the spectra of a non-degenerated Liouvillian.^{34–36} The idea is to observe universal features based on statistical correlations between the eigenvalues of the Liouvillian or the NESS. For closed Hamiltonian systems, there is a deep connection between the quantum chaos conjecture^{37,38} and the statistical correlations of the eigenvalues, which is described by random matrix theory.³⁹ However, for open quantum systems, very little is known in this direction.

For an open quantum system, there is a choice to study the spectral properties of either the Liouvillian or the steady-state density matrix. The spectral signatures of the Liouvillian reflect on the properties (e.g., localizing behavior) of *all* of its eigenmodes, most of

which are unphysical (trace zero operators) except the steady-state density matrix, whereas the study of spectral properties of the physically meaningful steady-state density matrix reflects on the properties of the eigenmodes of the steady-state density matrix. Moreover, for a complex many-body open quantum system, evaluating the entire spectra of the Liouvillian can be computationally expensive since its corresponding matrix dimension scales as $N^2 \times N^2$ (recall that N is the dimension of the system Hilbert space). For degenerated Liouvillians, most studies are restricted up to $N \approx 250$. On the other hand, since the NESS is the eigenvector corresponding to the zero eigenvalue of the Liouvillian, it can be obtained for much larger systems (up to $N \approx 1000$ provided the Liouvillian is sparse) using variants of the Lanczos algorithm. This reduces the computational cost of obtaining the NESS, but this reduction is accompanied by a square-root reduction in the sample size, which needs to be compensated by more sampling. In other words, the computational advantage of studying the eigenspacing statistics of the NESS lies in being able to explore large system Hilbert space to understand the scaling with N .

Although it is computationally lucrative to study the eigenspacing statistics of the NESS to uncover universal features, it is highly nontrivial if the Liouvillian is degenerated and the open system symmetries (weak or strong) are unknown. Without knowledge of the symmetry operators, the nonequilibrium steady states would be initial condition dependent, leading to a mixed NESS. The spectral statistics of such a mixed NESS would contain influences from all subspaces and hence would not give us a clear picture of the properties of the NESS in each subspace. Our approach based on orthonormalization (Sec. III B) is ideally suited to treat such cases since it helps obtain the steady state of each subspace without knowledge of the symmetry operators. To illustrate this idea, we consider the same *para*-benzene ring as before but choose the jump operators [Eq. (32)] extended to all ground-symmetric states $|i\rangle$ with $i = 1, \dots, 4$; see Eq. (34)] and then randomly picked from the Ginibre unitary ensemble.⁴⁰ To simulate a nonequilibrium situation, we choose only two jump operators $L_x/\sqrt{\Gamma_x}$ with $x = 1, 2$ whose distribution is given by

$$P(L_x) = \frac{1}{(2\pi)^{N^2}} \exp\left[-\frac{\text{Tr}[L_x^* L_x]}{2}\right], \quad (48)$$

with $N = 5$ for the case described above. This allows us to ensure that the randomization process is non-pathological⁴¹ and covers the manifold of all jump operators within the ground-symmetric subspace uniformly, as seen from the inset in Fig. 4, which shows the distribution of the eigenvalues of the Liouvillian. Moreover, the full Liouvillian still has a block-diagonal structure between ground-symmetric and anti-symmetric subspaces with three steady states. We use then our orthonormalization procedure outlined in Sec. III B and evaluate the distribution of the ratio of consecutive eigenspacing gaps,⁴²

$$0 \leq r_n = \frac{\min\{s_n, s_{n-1}\}}{\max\{s_n, s_{n-1}\}} \leq 1, \quad (49)$$

with $s_n = \nu_{n+1} - \nu_n$ being the eigenspacing of the NESS ($\rho^{\text{NESS}}|\varphi_n\rangle = \nu_n|\varphi_n\rangle$). The ratio, since it is independent of the local density of states, avoids irregularities due to finite-size of the NESS matrix and

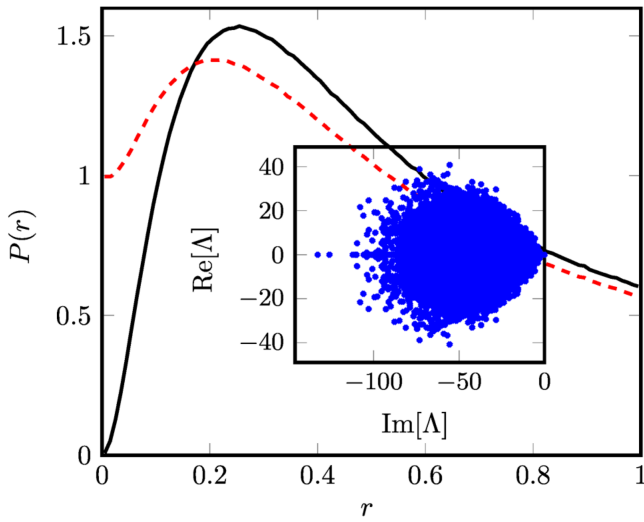


FIG. 4. The probability distribution $P(r)$ and the inset show the eigenvalues of the Liouvillian Λ confined to the ground-symmetric subspace. The solid black line shows the ratio of the eigenspacing gap distribution of the initial condition independent NESS obtained from the ground-symmetric subspace, whereas the red dashed line belongs to the distribution for the general mixed NESS, Eq. (50), averaged over 10^7 randomly chosen initial conditions, i.e., random c_i . The “lemon” shape⁴⁴ is distinct near the origin for the eigenvalues of the Liouvillian. The system Hamiltonian is chosen such that $J = 1$, and both distributions are averaged over 10^7 samples of the Lindblad jump operators. In the inset, we plot the eigenvalues only for 2500 randomly chosen samples. The jump operators have rates $\Gamma_L = 1$ and $\Gamma_R = 2$.

thus does not require the unfolding of the spectrum. The resulting distribution is shown by the black solid curve in Fig. 4. The distribution shows $P(r) \rightarrow 0$ as $r \rightarrow 0$, indicating level repulsion and/or spectral rigidity, which means that the NESS is a thermalizing or highly nonintegrable state; i.e., there exists no algebraic procedure to construct this state in a finite number of steps. The average $\langle r \rangle \sim 0.463$ lies in between the exact predictions from a Poisson ($\langle r \rangle \sim 0.386$) and a Gaussian orthogonal ensemble ($\langle r \rangle \sim 0.536$).⁴³ The inset, Fig. 4, shows the distribution of the eigenvalues of the Liouvillian, which are available in this case. It should be noted that a more sophisticated form of the sampling could be chosen to obtain a perfect lemon structure,^{34,44} but this does not turn out to be a strict requirement as indicated by the eigenspacing distribution of the NESS.

Moreover, if we do not restrict our investigation to the symmetric and ground state subspace, then our statistics will depend on the choice of the initial condition. The most general mixed form of the NESS that spans over the entire system Hilbert space reads

$$\rho_{\text{mix}}^{\text{NESS}} = c_1 \rho^{\text{NESS}} + c_2 \rho_1^{\text{DS}} + c_3 \rho_2^{\text{DS}}, \quad (50)$$

with ρ^{NESS} being the NESS in the ground and symmetric subspace and ρ_i^{DS} being the dark states given by Eq. (42). The coefficients c_i depend on the initial condition such that $\sum_i |c_i| = 1$. In order to eliminate the initial condition dependence, we further ensemble average over initial conditions by choosing c_i from a uniform

random distribution. The resulting distribution of the ratio of consecutive eigenspacing gaps of $\rho_{\text{mix}}^{\text{NESS}}$ is shown by the red dashed curve in Fig. 4. Clearly, we see a strong influence of the antisymmetric subspace on the distribution especially close to $r \rightarrow 0$. Such a strong influence is expected since our dimension of the antisymmetric subspace, whose asymptotic is a pure state, is comparable to the ground-symmetric subspace wherein the non-integrable NESS resides. Thus, in the case of degenerate Liouvillians, the spectral statistics of the NESS must be studied in each subspace independently (similar to the study of spectral statistics in closed systems in the presence of symmetries) such that all initial condition dependencies are eliminated, which could lead to spurious effects.

Overall, in this section, we studied the *para*-benzene ring in detail. Although we dealt with the symmetry-decomposition based approach (Sec. III A) throughout this section, we would like to end with a few remarks on the other two methods. In all cases, we found that the orthonormalization based approach (Sec. III B) yielded the same results as the symmetry-based one. The orthonormalization based approach was also able to treat the ideal-source case and obtain all the six steady states. In complex many-body systems wherein the symmetry operators are either not known or wherein there could be mechanisms due to the baths leading to additional steady states, the orthonormalization based approach is perfectly suited to treat such cases. The large deviation based approach although computationally cheap would fail in the equilibrium and ideal-source situation since the currents for all steady states are zero. This method would also not allow us to obtain the two dark states [Eq. (42)] from the anti-symmetric subspace since they both carry zero current. Finally, we ended with studying the eigenspacing distribution of the NESS using the orthonormalization based approach, which gave us the expected result that the NESS is a highly non-integrable state.

V. CONCLUSIONS

In this paper, we have presented several techniques to obtain the steady states of a degenerated Lindblad Liouvillian. Each method comes with advantages and disadvantages and, together, they form a useful toolbox for many different problems. First, we have presented a method based on the use of symmetry operators. This technique allows the analytical resolution of many systems, but it requires the existence and knowledge of the open system symmetry operators. The second method, based on a Gram–Schmidt orthonormalization is general and does not require knowledge about the symmetry operators, but it is computationally expensive. Its utility depends on the degree of degeneracy and on the system dimension. Finally, we have presented a method based on large deviations theory. It does not require any previous knowledge about the system symmetries, and it is also computationally cheap as it only requires the diagonalization of an operator of the same size as the Liouvillian. On the other hand, it only gives the density matrices that maximize or minimize a given flux.

These methods have been illustrated by a canonical example, a *para*-benzene ring. This system can be analytically diagonalized, and in several specific cases, it shows a rich phenomenology including dark states, oscillating coherences, and steady-states that

are not a consequence of symmetries. Finally, we have also studied the eigenspacing distribution of the NESS obtained via the orthonormalization method. Since the system by construction is a thermalizing open quantum system, the ratio of the eigenspacing gap distribution $P(r) \rightarrow 0$ as $r \rightarrow 0$.

There are still several open questions to be addressed in this field of research. The *para*-benzene ring considered herein had only one NESS, whereas the other steady states were pure. An interesting question remains whether it is possible to construct open quantum systems with more than one NESS, i.e., steady states influenced by the reservoir. Consequently, would these states belong to the same random matrix ensembles, and if they do not, what could be the consequences on observables such as heat and particle currents. Furthermore, the existence of trace zero steady-states has been recently probed,²² but the consequence of these states has not been analyzed so far. How they affect the physical properties of the system and how they can be engineered and detected remain open.

ACKNOWLEDGMENTS

J.T. acknowledges support by the Institute for Basic Science in Republic of Korea (No. IBS-R024-Y2). D.M. acknowledges the Spanish Ministry and the Agencia Española de Investigación (AEI) for financial support under Grant No. FIS2017-84256-P (FEDER funds). We would like to thank Sai Vinjanampathy for discussions and constructive comments on our manuscript.

DATA AVAILABILITY

The data that support the findings of this study are available from the corresponding author upon reasonable request.

REFERENCES

- ¹V. Gorini, A. Kossakowski, and E. Sudarshan, *J. Math. Phys.* **17**, 821 (1976).
- ²G. Lindblad, *Commun. Math. Phys.* **119**, 48 (1976).
- ³B. Olmos, I. Lesanovsky, and J. Garrahan, *Phys. Rev. Lett.* **109**, 020403 (2012).
- ⁴D. Manzano and E. Kyoseva, *Sci. Rep.* **6**, 31161 (2016).
- ⁵J. Han, D. Leykam, D. Angelakis, and J. Thingna, “Quantum transient heat transport in the hyper-parametric oscillator,” [arXiv:2011.02663](https://arxiv.org/abs/2011.02663) (2020).
- ⁶J. Thingna, M. Esposito, and F. Barra, *Phys. Rev. E* **99**, 042142 (2019).
- ⁷G. D. Chiara, G. Landi, A. Hewgill, B. Reid, A. Ferraro, A. Roncaglia, and M. Antezza, *New J. Phys.* **20**, 113024 (2018).
- ⁸J. Liu, D. Segal, and G. Hanna, *J. Phys. Chem. C* **123**, 18303 (2019).
- ⁹J. Q. Quach and W. J. Munro, *Phys. Rev. Appl.* **14**, 024092 (2020).
- ¹⁰A. Tejero, J. Thingna, and D. Manzano, *J. Phys. Chem. C* **125**, 7518 (2021).
- ¹¹M. Žnidarič, B. Žunkovič, and T. Prosen, *Phys. Rev. E* **84**, 051115 (2011).
- ¹²J. Thingna, J. García-Palacios, and J.-S. Wang, *Phys. Rev. B* **85**, 195452 (2012).
- ¹³A. Asadian, D. Manzano, M. Tiersch, and H. Briegel, *Phys. Rev. E* **87**, 012109 (2013).
- ¹⁴D. Manzano, C. Chuang, and J. Cao, *New J. Phys.* **18**, 043044 (2016).
- ¹⁵Z. Hu, R. Xia, and S. Kais, *Sci. Rep.* **10**, 3301 (2020).
- ¹⁶B. Kraus, H. Büchler, S. Diehl, A. Kantian, A. Micheli, and P. Zoller, *Phys. Rev. A* **78**, 042307 (2008).
- ¹⁷H. Breuer and F. Petruccione, *The Theory of Open Quantum Systems* (Oxford University Press, 2002).
- ¹⁸D. Manzano, *AIP Adv.* **10**, 025106 (2020).
- ¹⁹D. Evans and H. Hance-Olsen, *J. Funct. Anal.* **32**, 207 (1979).
- ²⁰B. Buča and T. Prosen, *New J. Phys.* **14**, 073007 (2012).
- ²¹D. Manzano and P. Hurtado, *Adv. Phys.* **67**, 1 (2018).
- ²²J. Thingna, D. Manzano, and J. Cao, *New J. Phys.* **22**, 083026 (2020).
- ²³S. Lieu, R. Belyansky, J. Young, R. Lundgren, V. Albert, and A. Gorshkov, “Symmetry breaking and error correction in open quantum systems,” *Phys. Rev. Lett.* **125**, 240405 (2020).
- ²⁴E. Fiorelli, P. Rotondo, M. Marcuzzi, J. Garrahan, and I. Lesanovsky, *Phys. Rev. A* **99**, 032126 (2019).
- ²⁵J. Thingna, D. Manzano, and J. Cao, *Sci. Rep.* **6**, 28027 (2016).
- ²⁶D. Manzano and P. Hurtado, *Phys. Rev. B* **90**, 125138 (2014).
- ²⁷T. Prosen and M. Žnidarič, *Phys. Rev. Lett.* **111**, 124101 (2013).
- ²⁸V. Albert and L. Jiang, *Phys. Rev. A* **89**, 022118 (2014).
- ²⁹T. Prosen, *Phys. Scr.* **86**, 058511 (2012).
- ³⁰Note that duality of basis ensures that the left and right eigenvectors form an orthonormal set. This does not ensure that the right eigenvectors are orthogonal among themselves.
- ³¹Z. Zhang, J. Tindall, J. Mur-Petit, D. Jaksch, and B. Buča, *J. Phys. A: Math. Theor.* **53**, 215304 (2020).
- ³²A. Hewgill, G. De Chiara, and A. Imparato, *Phys. Rev. Res.* **3**, 013165 (2021).
- ³³J. Thingna and J.-S. Wang, *EPL* **104**, 37006 (2013).
- ³⁴S. Denisov, T. Lapyteva, W. Tarnowski, D. Chruściński, and K. Życzkowski, *Phys. Rev. Lett.* **123**, 140403 (2019).
- ³⁵K. Wang, F. Piazza, and D. J. Luitz, *Phys. Rev. Lett.* **124**, 100604 (2020).
- ³⁶L. Sá, P. Ribeiro, and T. Prosen, *Phys. Rev. X* **10**, 021019 (2020).
- ³⁷M. Berry and M. Tabor, *Proc. R. Soc. Lond. A* **356**, 375 (1977).
- ³⁸M. Berry, *Ann. Phys.* **131**, 163 (1981).
- ³⁹M. Mehta, *Random Matrices* (Elsevier, New York, 2004).
- ⁴⁰J. Ginibre, *J. Math. Phys.* **6**, 440 (1965).
- ⁴¹T. Can, *J. Phys. A: Math. Theor.* **52**, 485302 (2019); see simple dissipator herein.
- ⁴²V. Oganesyan and D. A. Huse, *Phys. Rev. B* **75**, 155111 (2007).
- ⁴³Y. Y. Atas, E. Bogomolny, O. Giraud, and G. Roux, *Phys. Rev. Lett.* **110**, 084101 (2013).
- ⁴⁴The perfect lemon is achieved when the coherent contribution $-i[H, \rho]$ to the Liouvillian vanishes, which is not the case here.